

Chapter 5

Are there vibrations in nuclei?

Vibrations at low energy are considered from an historical and a global perspective. The most favored candidates for quadrupole vibrations, ^{110}Cd and its heavier neighbours, fail to match model patterns. The spectroscopic challenges of arriving at this view are emphasized. One-phonon octupole vibrations in spherical nuclei are sketched.

Concepts: harmonic vibrator model, quadrupole collectivity, octupole collectivity, spherical nuclei, liquid-drop models.

Learning outcomes: The key data view from this chapter is the illustration of how detailed spectroscopic data has cast doubt on the existence of low-energy quadrupole vibrations in nuclei. Notably, it is shown that studies of electric quadrupole matrix elements extending to the three-phonon level are essential—energy patterns alone have misled the nuclear structure community.

The issue of whether there are vibrations in nuclei divides into the occurrence of vibrations at low energy (0.5–10 MeV) and at high energy (10–40 MeV). High-energy vibrations in nuclei are unequivocal, they are the so-called giant resonance modes. They are resonances, i.e. they are not energy eigenstates, because they occur above the threshold for nucleon emission and lack centrifugal or Coulomb barriers for at least one decay channel. Low-energy vibrations have had a mixed reception as a recognized collective mode in nuclei. We present a description of the giant resonance modes later in the Series. Immediately one must subdivide the topic of low-energy vibrational modes in nuclei into the study of spherical nuclei and the study of deformed nuclei. As with rotations, it is essential to adopt guidance from simple models. Such models differ substantially between those for spherical nuclei and those for deformed nuclei. Herein, we limit ourselves to the simplest possible spherical models. We address vibrations in deformed nuclei in the following chapter.

5.1 Historical view of low-energy vibrations in nuclei

The idea that nuclei support low-energy vibrational modes originated with the seminal work of Aage Bohr in 1952 [1]. Bohr proposed a liquid drop model of the nucleus, which could be spherical and exhibit quantized vibrations, or it could deform and exhibit quantized rotations and vibrations.

Experimental data in support of low-energy quadrupole vibrations in nuclei was published already in 1955 by Gertrude Scharff-Goldhaber and Joseph Weneser [2]. This view was broadened in 1960 by Raymond Sheline [3] with an assessment of evidence for low-energy vibrations in deformed nuclei, albeit with a severe lack of useful data for the task.

The simplest model of vibrations is depicted in figure 5.1. This treats the nucleus as a uniform liquid drop with a sharp surface. This droplet of fluid can deform, maintaining constant density. The excitations have a simple ‘phonon’ structure and are equidistantly spaced. More subtly, the transition strength from the two-phonon state to the one-phonon state is twice the strength from the one-phonon state to the ground state. The transition strength rule follows from the elementary quantum mechanics of the one-dimensional simple harmonic oscillator, expressed in algebraic terms, viz.

$$a^\dagger |0\rangle = |1\rangle \quad (5.1)$$

$$a^\dagger |n\rangle = \sqrt{n+1} |n+1\rangle \quad (5.2)$$

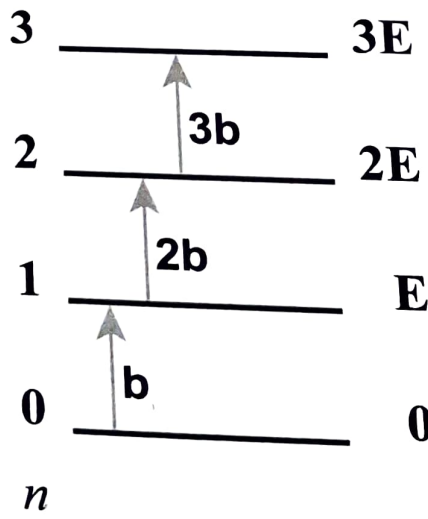


Figure 5.1. Schematic view of a quantum mechanical harmonic vibrator. The excitations are characterized by equidistant spacing of energy levels: this is well known from the elementary nature of the quantum mechanical one-dimensional harmonic oscillator. The transition strengths are characterized by a monotonic increase between these levels: this is less-well known, and the reason is presented in the algebra shown in the text. The only labelling quantum number at this level of detail is n , the number of oscillator ‘phonons’. The transition strengths are expressed as matrix elements, which are proportional to the operator connecting the states. Note, the transitions are shown as excitations, but the matrix elements are the same for de-excitation.

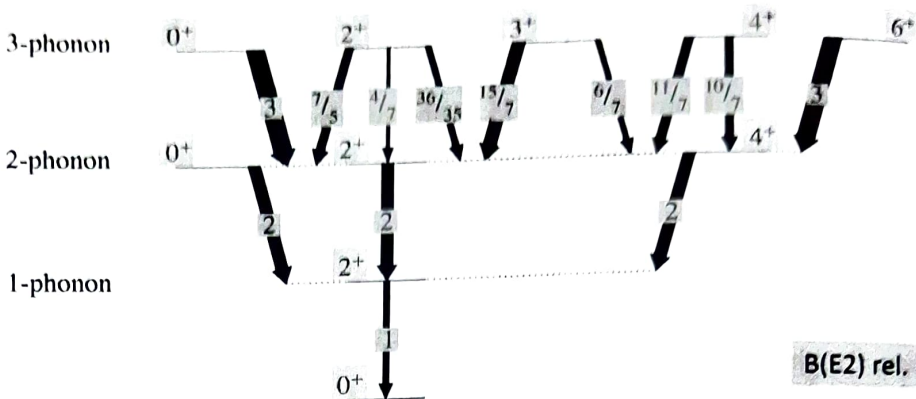


Figure 5.2. Schematic view of the harmonic quadrupole vibrator, i.e. for oscillator phonons carrying a spin of 2. Such phonons are bosons and the allowed total spins for multi-phonon coupling are determined using the m-scheme (see exercises 5-1 and 5-2). The transition strengths follow the naïve view presented in figure 5.1 up to the two-phonon level, but at the three-phonon level the $n = 3 \rightarrow n = 2$ transition strengths reflect partitioning due to the spin structure of the phonons, which is beyond the present level of discussion (note that the partitions sum to three units of oscillator strength for each member of the three-phonon quintuplet).

$$T(n \rightarrow n + 1) = b \langle n + 1 | a^\dagger | n \rangle^2 = b(n + 1) \quad (5.3)$$

For spherical nuclei, the leading order vibrational mode is quadrupolar and this is depicted in figure 5.2. This mode is treated as a harmonic oscillator with quanta carrying a spin of two. Thus, the one-phonon excitation has spin 2, and two-phonons of excitation result in three excited states with spins¹ 0, 2 and 4. The two-phonon triplet forms a degenerate multiplet at twice the energy of the one-phonon excitation. Figure 5.2 provides a useful view of the key energy signatures and $B(E2)$ signatures for assessing low-energy quadrupole vibrational modes in nuclei. Specifically, candidate nuclei should exhibit $E(4_1)/E(2_1) \sim 2$ and $B_{42}/B_{20} \sim 2$. There appear to be some candidates. Indeed, based on these two criteria, together with the phonon selection rule which dictates that $B_{2'0}/B_{2'2} \sim 0$, an extensive body of literature developed such that it was widely accepted: ‘nuclei near closed shells are spherical and exhibit low-energy quadrupole vibrations’. However, little attention was paid to the requirement that $B_{2'2} \sim 2B_{20}$ and $B_{0'2} \sim 2B_{20}$. This lack of attention was rationalized on the basis that lifetime measurements in the ps–ns range had to be made. Such measurements are, in general, not easy. Further, $2' \rightarrow 2$ transitions necessitated the determination of the $E2/M1$ mixing ratio for the transition. This required $\gamma\gamma$ angular correlation measurements, i.e. coincidence measurements as a function of the angle between two detectors. Again, such measurements are not easy. Yet further was the impediment that excited 0^+ states are difficult to populate, especially using in-beam methods where lifetime information is accessible by Doppler shift methods.

¹ See exercise 5-1 for the use of the m-scheme (for bosons) applied to the deduction of these spins for the two-phonon multiplet. Also see exercise 5-2 for the deduction of spins 0, 2, 3, 4, 6 for the three-phonon multiplet.

The above view prevailed for fifty years. It is fair to say that there was universal satisfaction with this view being correct. In the early 2000s a program at University of Kentucky was underway to characterize the best candidate nuclei for harmonic quadrupole vibrations. There were 'textbook' cases: ^{110}Cd was a favoured example [4]. The studies at University of Kentucky focussed on gamma-ray spectroscopy following inelastic scattering of neutrons from $^{110,112,114,116}\text{Cd}$. These studies provided a comprehensive view of the low-energy excitations and, most importantly, lifetime information in the 30–700 fs range from Doppler energy shifts of gamma rays. The revelation came with respect to the candidate states for three-phonon excitations: the expected 3-phonon \rightarrow 2-phonon $B(E2)$ strength, which should sum to $3B_{20}$, was not realized in these nuclei. This turned an optimistic exploration of low-energy harmonic quadrupole vibrations into a realization that the concept was questionable, i.e. low-energy multi-phonon excitations may not exist in nuclei for quadrupole excitations. Key steps in this saga are described in [5, 6]. We look at the pros and cons for low-energy quadrupole vibrations in nuclei in the next section.

5.2 Assessment of low-energy quadrupole vibrations in nuclei

The isotopes $^{110,112,114,116}\text{Cd}$ are generally considered the textbook example of low-energy quadrupole vibrations in nuclei. The details of $E2$ transition strengths between the low-energy excited states in $^{110,112,114}\text{Cd}$ are presented, in comparison to the pattern in figure 5.2, in figures 5.3(a)–(d). The most problematic feature for a vibrational interpretation is the extremely weak $B(E2)$ value from the candidate 2-phonon 0^+ state to the 1-phonon (2^+) state in $^{112,114}\text{Cd}$. Further, the $B(E2)$ values from the candidate 3-phonon 2^+ state to the candidate 2-phonon 2^+ and 4^+ states are very weak in all three isotopes. Indeed, one notes that the candidate 3-phonon 2^+ state exhibits a strong $B(E2)$ value to the candidate 2-phonon 0^+ state in all three isotopes: this identifies the two states, unequivocally in $^{112,114}\text{Cd}$ and by implication in ^{110}Cd , as forming the beginning of a band structure. This band is manifestly isolated from all the other low-energy states in all these isotopes.

Figures 5.4(a)–(d) shows a rearrangement of the states depicted in figures 5.3(a)–(d), together with the low-energy shape coexisting, intruder states, cf 3.22, to reflect evident multiple band structures in $^{110,112,114}\text{Cd}$. Most notably, the $B(E2)$ values support the beginning of a $K = 2$ band, constituted from the candidate 2-phonon 2^+ state and the candidate 3-phonon 3^+ and 4^+ states. The ground state is the head of a $K = 0$ band and the above-noted newly emerging band can be interpreted as having a $K = 0$ and is very similar to the ground-state band. The shape-coexisting states form a $K = 0$ band as already identified in 3.22. Yet further, as shown in 4.37, ^{114}Cd exhibits the characteristics of $K = 2$ coexisting bands, and the present identification sharpens the view of the lowest $K = 2$ band. We particularly note that $E0$ transitions play a key role in this structural identification: $E0$ transitions cannot change K and a $\Delta K = 0$ selection rule is evident for the patterns of $E0$ transitions in 4.37. As a capstone perspective on this rearrangement to the low-energy structure of the even Cd isotopes, figures 5.5(a) and (b) shows the population of low-lying states in $^{108,110}\text{Cd}$ by the $^{107,109}\text{Ag}(\text{He},\text{d})$ reaction. Evidently, the 0^+ state in ^{110}Cd that

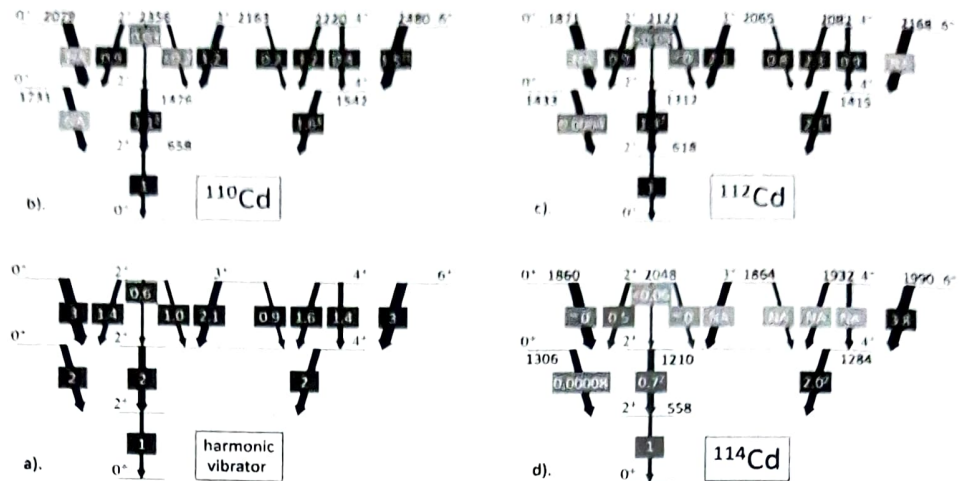


Figure 5.3. States that are candidates for quadrupole vibrational behaviour in $^{110,112,114}\text{Cd}$. The data are arranged to match the pattern shown in figure 5.2, which is repeated in frame (a). Frames (b), (c), and (d) summarize currently available data for ^{110}Cd , ^{112}Cd and ^{114}Cd , respectively. Energies are given in keV and $E2$ transition strengths are given relative to $B(E2; 2_1^+ \rightarrow 0_1^+) = B_{20} = 1.00$; the B_{20} values in W.u. (from ENSDF) are 27.08 (^{110}Cd), 30.32 (^{112}Cd) and 31.2 (^{114}Cd). Transitions for which data are not available are labelled 'NA'. Severe departures from expectations for harmonic quadrupole vibrational behaviour are highlighted in red; note that these exhibit a systematic pattern.

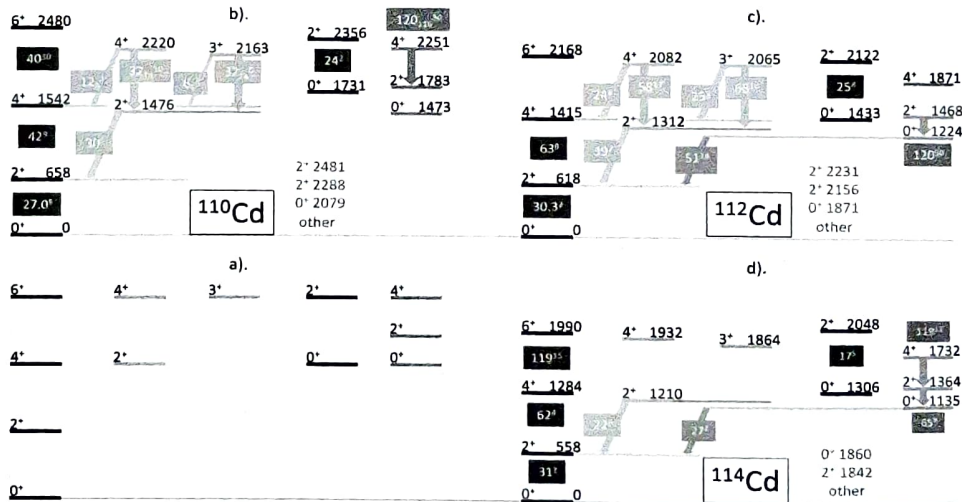


Figure 5.4. Low-energy excited states in $^{110,112,114}\text{Cd}$ arranged into band patterns and contrasted with a harmonic quadrupole vibrator view. The data are arranged to match the pattern shown in figure 5.2, which is rearranged in frame (a). Frames (b), (c), and (d) summarize currently available data for ^{110}Cd , ^{112}Cd and ^{114}Cd , respectively. Energies are given in keV. The $E2$ transition strengths are given in W.u. and are shown only for strong transitions, where known. Colour coding is simply to assist in recognizing the groupings of the $E2$ transitions. Other, lowest positive-parity excited states that are omitted are listed by energy. The bands conform to patterns for $K = 0, 2$ and are discussed further in the text. The data are taken from ENSDF and the $B(E2)$ values are rounded to essential significant figures.

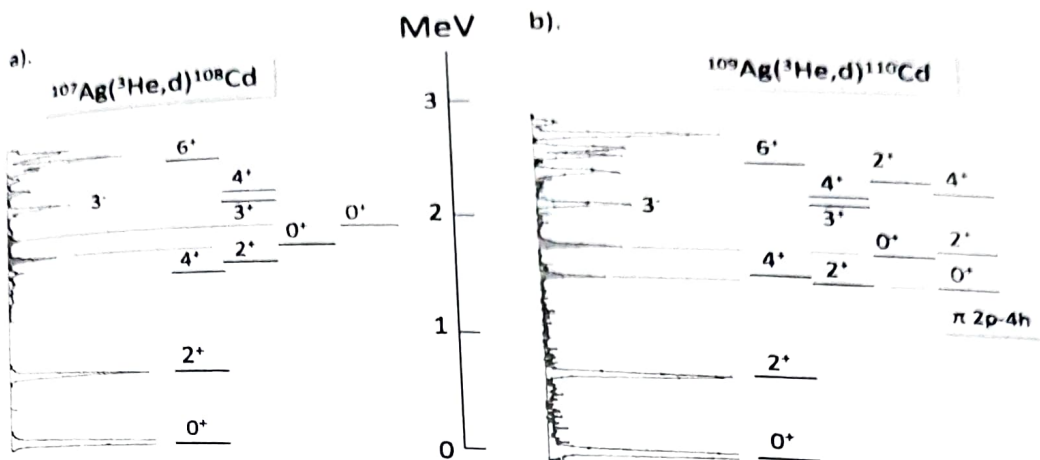


Figure 5.5. States in $^{108,110}\text{Cd}$ populated in the $^{107,109}\text{Ag}(^3\text{He},d)^{108,110}\text{Cd}$ one-proton transfer reaction. The spectra of proton ejectiles are matched to the low-energy excited states in the final nuclei, arranged into K bands as in figure 5.4, with excited 0^+ states highlighted in red. Note that the one-proton transfer strength is fragmented between the intruder $K = 0$ band head, labelled $\pi 2p-4h$, and the head of the $K = 0$ band proposed states in figure 5.4, with somewhat more strength to the proposed (non-intruder) band. Population of first excited 3^- states is indicated. Other features in the proton ejectile spectra involve excited states which are not relevant to the present discussion. Further details are discussed in the text. The data are taken from [7] and from ENSDF.

has been considered as a 2-phonon state has long been known to have significant proton excitation character, possibly a redistribution of $J = 0$ proton pairs within the $1g_{9/2}-2p_{1/2}$ subshells.

A further feature of these cadmium isotopes is that the 2_1^+ states are observed to have non-zero quadrupole moments, viz. -0.40^3 b (^{110}Cd); -0.38^3 b (^{112}Cd); -0.35^5 b (^{114}Cd), cf ENSDF. These values imply that the cadmium isotopes are deformed. Historically, these values were addressed as evidence of anharmonic vibrations. We do not consider such descriptions of the cadmium isotopes herein because of the complexity of such descriptions of nuclei. The present view is strictly for harmonic quadrupole vibrations of spherical nuclei, for which $Q = 0$ for all states.

The data presented here capture the essential steps in the historical realization [5, 6] that these Cd isotopes do not provide a textbook example of low-energy quadrupole vibrational behaviour. To the contrary, they exhibit quasi-rotational bands that can be labelled by K quantum numbers. Thus, the title of this chapter comes into focus. One way forward is suggested by the details presented in figure 5.1: one must thoroughly characterize the $E2$ transitions in nuclei with $R_4 \sim 2.0$ and $B_{42}/B_{20} \sim 2.0$. Figures 5.6(a) and (b) present a comprehensive view of R_4 and B_{42} versus B_{20} for all nuclei with $B_{20} < 100$ W.u.

The challenge to exploring excited states in nuclei such as $^{110-116}\text{Cd}$ is the assignment of higher lying states into bands or multi-phonon multiplets. The issue is the difficulty in determining the intensities of low-energy transitions between high-lying states. This is due to the ever-present issue of the E_γ^5 factor in observed $E2$

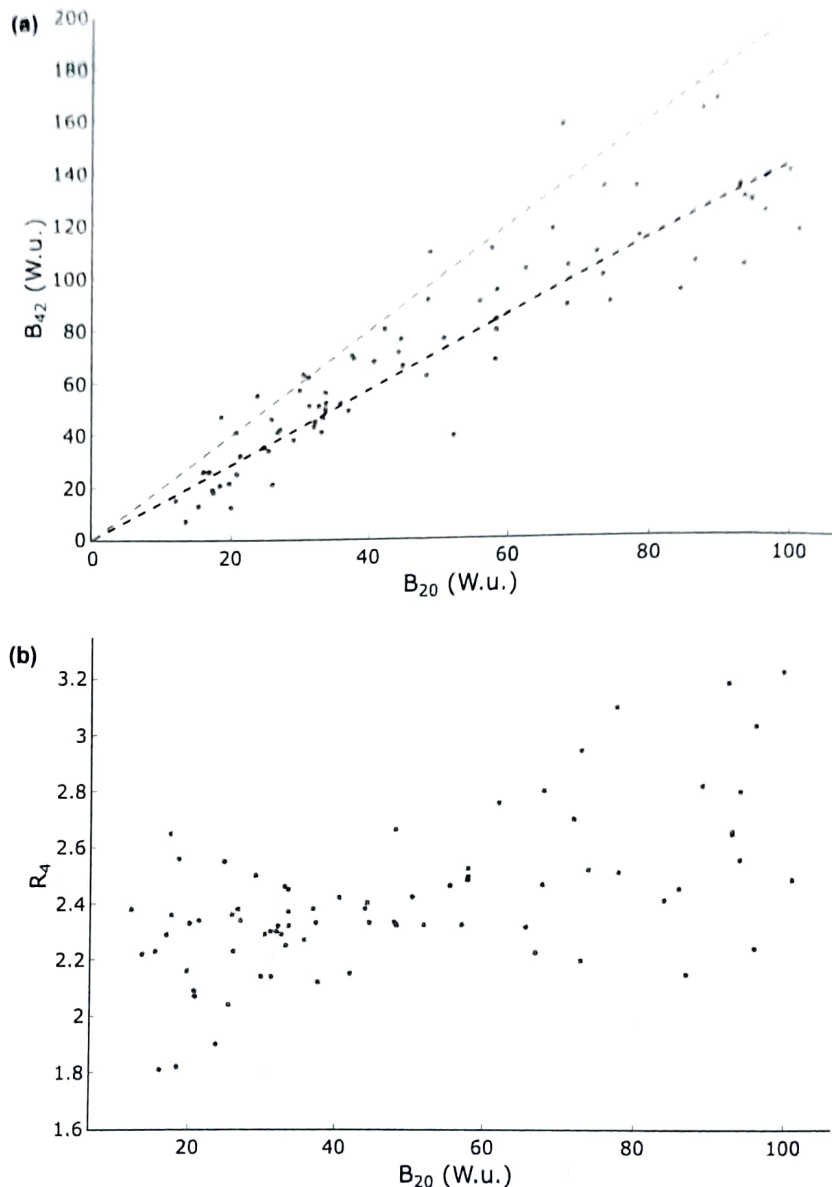


Figure 5.6. (a) Plot of B_{42} versus B_{20} for all nuclei with $B_{20} < 100$ W.u. The red dashed line indicates the expected trend for vibrational nuclei while the black dashed line indicates the expected trend for rotational nuclei. (b) Plot of R_4 versus B_{20} for all nuclei with $B_{20} < 100$ W.u. The limit of 100 W.u. on B_{20} is arbitrarily set as a lower limit for nuclei that might be considered to possess collective rotations; thus, the nuclei included in these plots should cover all cases where collective vibrations might be considered as manifested. Error bars are suppressed for clarity of presentation but the reader should bear in mind that many of transition strengths, in particular, have significant uncertainty. (Interactive version available for e-book can be downloaded from <http://iopscience.iop.org/book/mono/978-0-7503-5643-5>.)

transition decay rates. An example is shown in figure 5.7. The only solution is to take data using large arrays of detectors running for very long data acquisition times at very high counting rates. All three of these factors have limitations: cost of detectors, human cost in working hours, equipment sharing limitations, event acquisition-rate

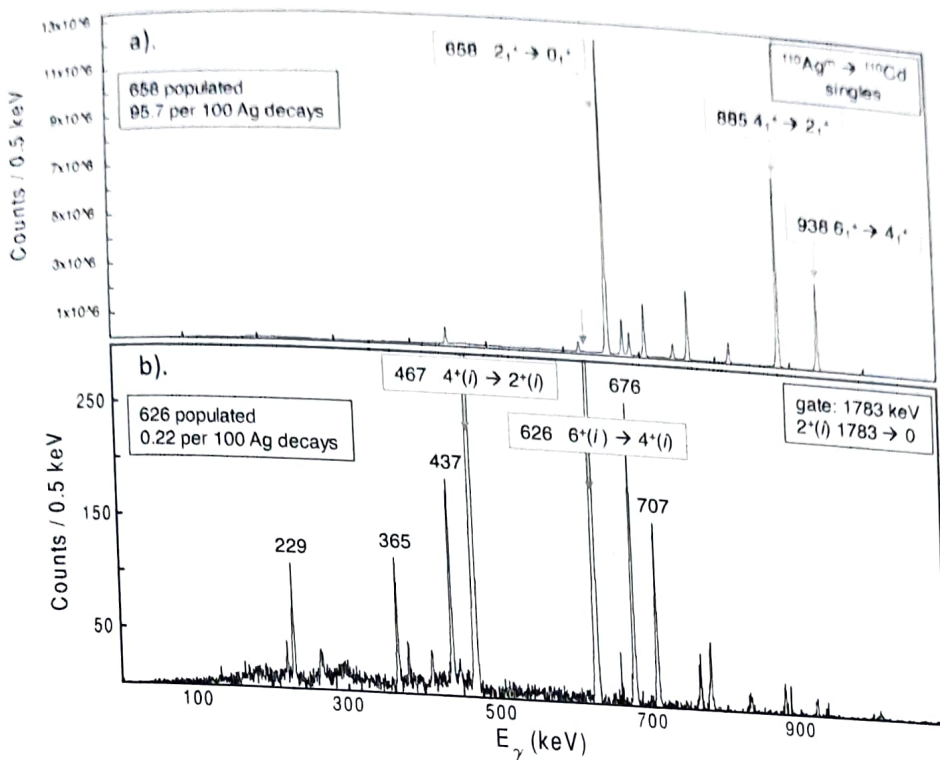


Figure 5.7. Illustration of the observation and quantification of very weak decay branches in the nucleus ^{110}Cd following the radioactive decay $^{110}\text{Ag}^m$ (β^- , $T_{1/2} = 249.83$ d, $J^\pi = 6^+$, $Q_\beta = 2891$ keV). These weak decay branches occur uniformly between excited states in all nuclei, where the E_γ^5 factor, inherent in $E2$ transition rates, dominates radiative decay. (a) The singles spectrum shows identification of some strong transitions, cf the figure 5.4(b); the red arrow shows the barely visible 626 keV peak. (b) Spectrum of γ rays in coincidence with Notably, the spectrum shows a 467 keV γ ray which supports the intruder band structure shown in figure 5.4(b) (and see 3.22). The 1783 keV γ -ray transition occurs 1.02×10^{-4} per $^{110}\text{Ag}^m$ β decay. The 467 keV γ ray occurs 2.5×10^{-4} per $^{110}\text{Ag}^m$ β decay yet corresponds to a transition with a strength of 120_{110}^{50} W.u. The spectrum shows many other γ -ray lines corresponding to transitions which feed the 1783 keV state directly and indirectly. The figure is provided courtesy of J M Allmond and the data were acquired in a 200 day data collection with the CLARION array at Oak Ridge National Laboratory. The figure is similar to one in [8].

limitations of electronics. *This aspect of nuclear spectroscopic study has become one of the major limitations to advancing our understanding of nuclear structure.* We address the other limitations shortly.

It is evident that what is needed, to advance our understanding of nuclei such as the Cd isotopes and their collectivity, is a ‘map’ of the electric quadrupole excitation response such as can be achieved in multi-step Coulomb excitation. This is illustrated in figure 5.8. With respect to the ‘ E_γ^5 problem’, there is a positive view. This factor applies to the spontaneous radiative decay of the state in question; it does not apply to Coulomb excitation. While one observes the result of Coulomb excitation via the relaxation of the nucleus back to the ground state by spontaneous radiative decay, these gamma-ray yields are deconvoluted into what happened in the multi-step excitation paths. In such paths, low-energy collective transitions have a

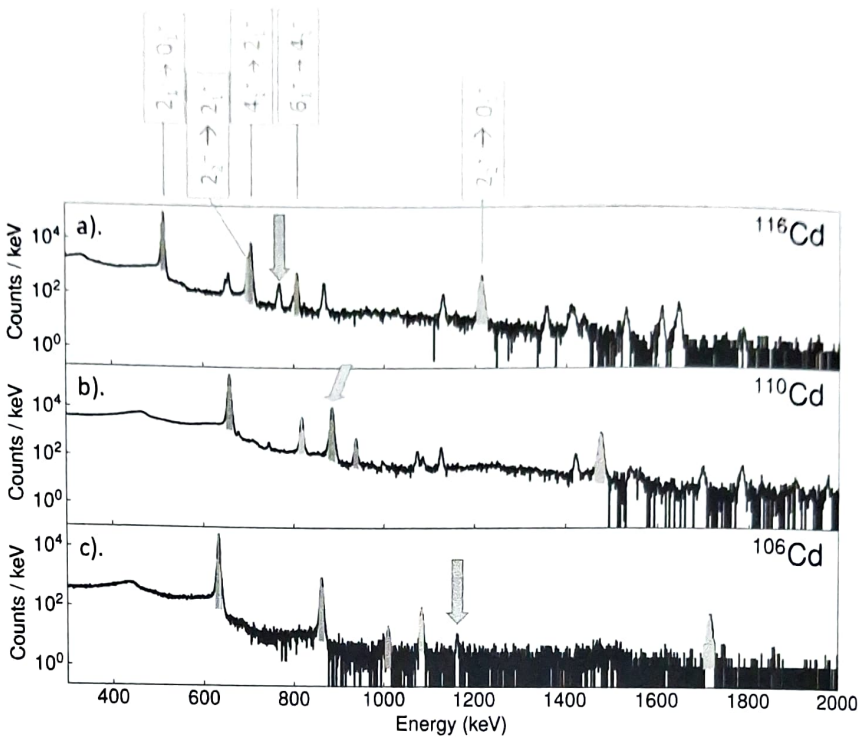


Figure 5.8. Coulomb excitation of $^{106,110,116}\text{Cd}$ beams on a ^{208}Pb target, observed via γ -ray spectroscopy. The spectra shown, (a) ^{116}Cd , (b) ^{110}Cd and (c) ^{106}Cd , were obtained under identical conditions, thus permitting a direct comparison of the multi-step electromagnetic responses of these nuclei. The transitions assigned to the observed strong γ rays are shown, of figure 5.4(b) (and 3.22) for ^{110}Cd . The (locations of) $0_2^+ \rightarrow 2_1^+$ transitions are indicated with bold orange arrows. Note that the $2_2^+ \rightarrow 2_1^+$ and $0_2^+ \rightarrow 2_1^+$ transitions are an unresolved doublet in ^{110}Cd . Other γ -ray lines in the spectra are considered in exercise 5-7. The figure is provided courtesy of T J Gray and J M Allmond. The data were acquired with GRETINA-CHICO-2 at Argonne National Laboratory. The data for ^{106}Cd are presented in [9].

high probability, with a much less sensitive dependence on how far removed they are from the ground state (but ultimately only a finite number of excitation steps occur in an experiment).

A feature of multi-step Coulomb excitation studies, that can be confusing to the inexperienced eye, is the deduction of strengths ($E2$ matrix elements) for transitions that are not observed. The reason they are not observed is because observation is via relaxation after the Coulomb excitation process; this is via the process of spontaneous emission which is subject to the E_γ^5 factor. The reason they can be deduced is because they play a dominant role in the Coulomb excitation process. A dramatic manifestation of this is the population of negative-parity states: the excitation mode is via $E3$ matrix elements, the de-excitation mode is via $E1$ radiative decay. Excitation by $E1$ matrix elements has low probability because such matrix elements for nuclei are very small between low-energy states; de-excitation by $E3$ radiative decay has low-probability because coupling to the EM vacuum is weak due to the high spin change.

5.3 Low-energy octupole vibrations in spherical nuclei

Octupole vibrations in nuclei have been a topic of much less interest than quadrupole vibrations, because they are not dominant. There is a candidate one-phonon octupole state in most even-even nuclei if that nucleus has been studied in any detail. A map of excitation energies of 3^-_1 states is shown in figure 5.9. The $B(E3)$ strength associated with the 3^-_1 states in figure 5.9 is shown in figure 5.10. Such excitations are directly observed by inelastic scattering. Examples are shown for the double-closed shell nucleus, ^{208}Pb in figure 5.11 and for the single-closed shell nucleus, ^{118}Sn in figure 5.12. Note there is a major review of this topic [10].

The question of the existence of two-phonon octupole excitations remains elusive. Two technical factors are: they will have excitation energies where the level density is high and they will have positive parity; therefore, they will be difficult to characterize against a ‘background’ of many excited states, many poorly characterized, and they will decay by transitions with $E2$ and $M1$ multipolarity. There has been some interest in excitations described as one-phonon quadrupole coupled to one-phonon octupole, notably in the Cd isotopes. But such excitations are now in question, based on details given in section 5.2.

The occurrence of octupole collectivity as a function of N and Z does not match liquid drop descriptions. A liquid drop should exhibit the lowest energy and highest strength for a collective excitation far from closed shells where the nucleus is least ‘rigid’. This indicates that octupole collectivity is controlled by properties of proton and neutron configurations. This point is visited in detail for deformed nuclei.

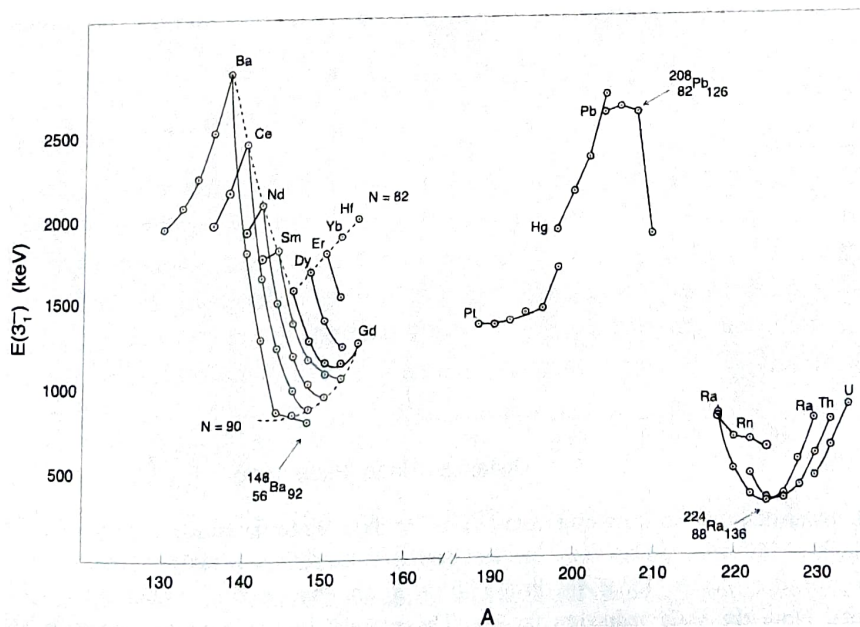


Figure 5.9. Systematics of the energies of the first excited states with spin-parity 3^-_1 for $56 \leq Z \leq 64$, $78 \leq Z \leq 82$, and $88 \leq Z \leq 92$. Isotopes are joined by solid lines and isotones by dashed lines. The data are taken from [10]. The figure is reproduced from [11], copyright 2010 World Scientific Publishing Company.

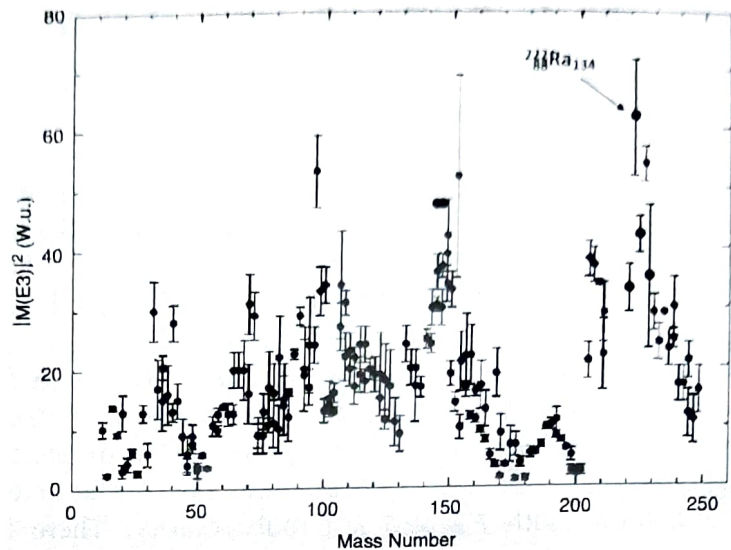


Figure 5.10. Systematics of electric octupole transition strength $|M(E3)|^2$ between the ground state and first excited 3^- state in doubly-even nuclei. The $|M(E3)|^2$ values are in Weisskopf units, W.u. The figure provides an update to data earlier presented in [10]. The figure is reproduced from [11], copyright 2010 World Scientific Publishing Company.

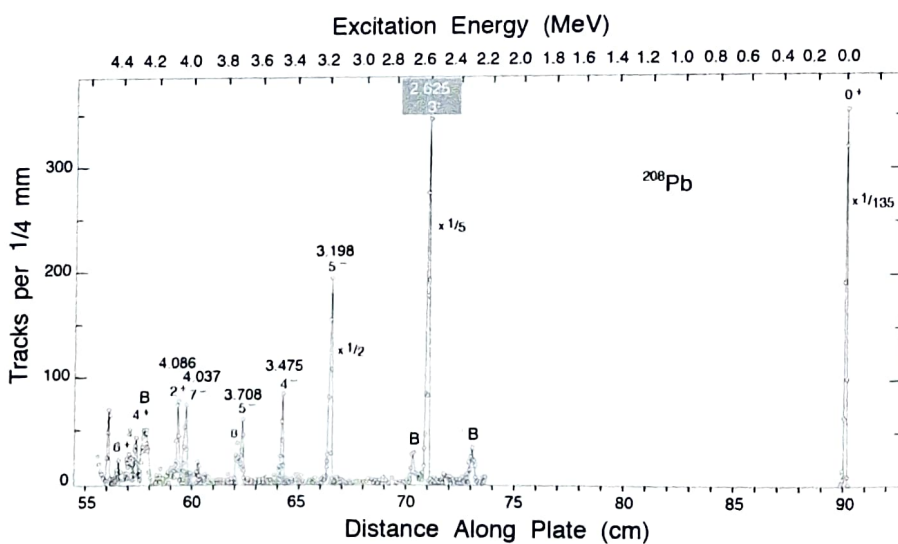


Figure 5.11. Inelastic deuteron scattering from ^{208}Pb . The data are for an incident energy of 13.1 MeV and a scattering angle of 150° with respect to the incident beam. Deuteron lines are labelled by the spins and parities of the corresponding levels. Lines marked with a B are ‘background’ events resulting from target contaminants. Note the scale reduction factors. The energies and spin-parities are from ENSDF. The figure is reproduced from [11], copyright 2010 World Scientific Publishing Company.

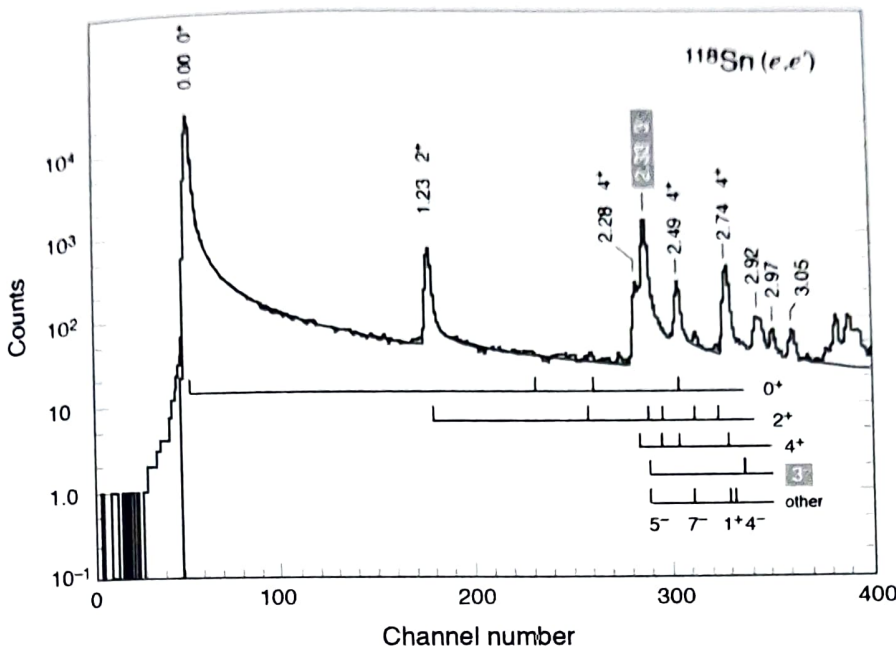


Figure 5.12. Inelastic electron scattering from ^{118}Sn . The data are for an incident energy of 252 MeV and a scattering angle of 68° with respect to the incident beam. The peaks corresponding to excited states reveal those states which are connected to the ground state by the largest electromagnetic matrix elements. The $I^\pi = 2^+$ state at 1.23 MeV and the $I^\pi = 3^-$ state at 2.33 MeV are deduced to be excited by strong electric quadrupole and electric octupole processes, respectively. The location of other excited states in ^{118}Sn is indicated; spins, parities, and excitation energies (in MeV) are taken from ENSDF. The figure is discussed further in the text. Reprinted figure with permission from [12], copyright 1991 by the American Physical Society.

5.4 Exercises

- 5-1. Deduce allowed spins for two spin-2 bosons using the m scheme.
- 5-2. Repeat exercise 5-1 for three spin-2 bosons.
- 5-3. Using the algebra presented in equations (5.1)–(5.3), show that a $n \rightarrow n - 2$ transition is impossible within the harmonic vibrator model (cf figure 5.1).
- 5-4. Deduce allowed spins for two spin-3 bosons using the m scheme.
- 5-5. With reference to figures 5.3 and 5.4, using data in ENSDF, as far as possible, classify excited states in
 - (a) $^{118,120,122}\text{Te}$;
 - (b) $^{104,106,108}\text{Pd}$.
- 5-6. Make use of data in ENSDF to identify candidate nuclei with $J = 0, 2, 4$ triplets which lack lifetime data.
- 5-7. With reference to figure 5.8, using data in ENSDF, identify the γ -ray lines in the spectra associated with the decays of:
 - (a) the 3_1^- states;
 - (b) the 0_3^+ states;
 - (c) other states in ^{116}Cd .